MOLECULAR AND CELLULAR BIOLOGY, Feb. 2004, p. 1667–1679 Vol. 24, No. 4
0270-7306/04/$08.00+0 DOI: 10.1128/MCB.24.4.1667–1679.2004

Placental Failure and Impaired Vasculogenesis Result in Embryonic Lethality for Neuropathy Target Esterase-Deficient Mice

Markus Moser,[1]* Yong Li,[2] Kristina Vaupel,[1] Doris Kretzschmar,[3] Reinhart Kluge,[4] Paul Glynn,[2] and Reinhard Buettner[5]

Max Planck Institute for Biochemistry, D-82152 Martinsried,[1] Max Rubner Laboratorium, German Institute of Human Nutrition, D-14558 Bergholz-Rehbrücke,[4] and Institute of Pathology, University Bonn, D-53127 Bonn,[5] Germany; MRC Toxicology Unit, University of Leicester, Leicester LE1 9HN, United Kingdom[2]; and Center for Research on Occupational and Environmental Toxicology L606, Oregon Health and Sciences University, Portland, Oregon 97201-3098[3]

Received 19 March 2003/Returned for modification 26 April 2003/Accepted 21 October 2003

Age-dependent neurodegeneration resulting from widespread apoptosis of neurons and glia characterize the *Drosophila* Swiss Cheese (SWS) mutant. Neuropathy target esterase (NTE), the vertebrate homologue of SWS, reacts with organophosphates which initiate a syndrome of axonal degeneration. NTE is expressed in neurons and a variety of nonneuronal cell types in adults and fetal mice. To investigate the physiological functions of NTE, we inactivated its gene by targeted mutagenesis in embryonic stem cells. Heterozygous NTE$^{+/-}$ mice displayed a 50% reduction in NTE activity but underwent normal organ development. Complete inactivation of the NTE gene resulted in embryonic lethality, which became evident after gastrulation at embryonic day 9 postcoitum (E9). As early as E7.5, mutant embryos revealed growth retardation which did not reflect impaired cell proliferation but rather resulted from failed placental development; as a consequence, massive apoptosis within the developing embryo preceded its resorption. Histological analysis indicated that NTE is essential for the formation of the labyrinth layer and survival and differentiation of secondary giant cells. Additionally, impairment of vasculogenesis in the yolk sacs and embryos of null mutant conceptuses suggested that NTE is also required for normal blood vessel development.

Neuropathy target esterase (NTE) was originally identified by its reactivity with specific organophosphates (OP), which in adult humans and some other vertebrates cause delayed neuropathy (14). This syndrome is characterized morphologically by degeneration of large axons in the peripheral nerves and spinal cord and clinically by paralysis of the lower limbs (5). Within the adult vertebrate nervous system, NTE is expressed in neurons, particularly strongly in those with large cell bodies, and can undergo fast axonal transport (10, 23). The link between OP-mediated modification of NTE and onset of neuropathy is obscure. Although this syndrome may reflect a requirement for NTE to maintain axonal integrity, it is also possible that it is caused by the gain of a novel toxic function in OP-modified NTE rather than by loss of NTE's normal activity (11).

Clear evidence for a role of NTE function in neural integrity comes from analysis of *Drosophila* carrying mutant versions of NTE homologue Swiss Cheese (SWS). Mutations in the *sws* gene resulted in age-dependent neurodegeneration, massive apoptosis, and early death (17). The earliest morphological abnormality detected in the mutant flies was hyperwrapping of glial membrane sheets around neuronal cell bodies and axons. SWS expression was detected in most neurons, and it seemed possible that this protein was involved in neuron-glia interactions during development of the fly brain (17). Similarly, NTE mRNA is strongly expressed in neural ganglia in mice by embryonic day 13 postcoitum (E13), consistent with a possible role for NTE in vertebrate neural development (23).

The distribution of NTE in tissue suggests that this protein may have, in addition to potential vital roles in the nervous system, more-general functions. As judged by esterase assays and Northern blotting, NTE is expressed in a variety of adult vertebrate tissues including gut, lymphocytes, skeletal muscle, kidney, and placenta, as well as in brain (16, 20). Similarly, during mouse embryogenesis, in situ hybridization reveals widespread expression of NTE in a number of ectoderm-, mesoderm-, and endoderm-derived tissues (23). In this article we demonstrate that NTE is essential for the formation of extraembryonic tissues, especially the placenta, and that its elimination results in massive cell death within the embryo.

MATERIALS AND METHODS

Isolation of the murine NTE gene locus and construction of the targeting vector. A commercially available murine 129/Sv genomic library (lambda FixII; Stratagene, Heidelberg, Germany) was screened with a randomly labeled NTE cDNA fragment spanning nucleotides 1175 to 2575 (23) by standard procedures (24). DNA sequencing was performed by cycle sequencing using an automatic DNA sequencer (Applied Biosystems, Boulder, Colo.). A positive 17-kb clone spanning five exons encoding nucleotides 1105 to 1709 of the murine cDNA (NM_015801) (23) was analyzed by restriction mapping, and fragments were subcloned into pBluescript. The targeting vector was constructed by inserting a β-gal-neo cassette into the *Eco*RV site at bp 1406 of NTE cDNA corresponding to amino acid 397 (relative to the start site of translation). This mutation causes premature protein truncation prior to the carboxyl-terminal catalytic domain. For electroporation the vector was linearized with the restriction enzyme *Sal*I.

Gene targeting in ES cells and generation of gene-disrupted mice. Sixty micrograms of linearized plasmid DNA was electroporated into 4×10^7 R1 embryonic stem (ES) cells suspended in phosphate-buffered saline (PBS). Transfection of and culture conditions for ES cells were as described previously (22).

* Corresponding author. Mailing address: Max Planck Institute for Biochemistry, Am Klopferspitz 18A, D-82152 Martinsried, Germany. Phone: 49 89 8578 2849. Fax: 49 89 8578 2422. E-mail: moser@biochem.mpg.de.

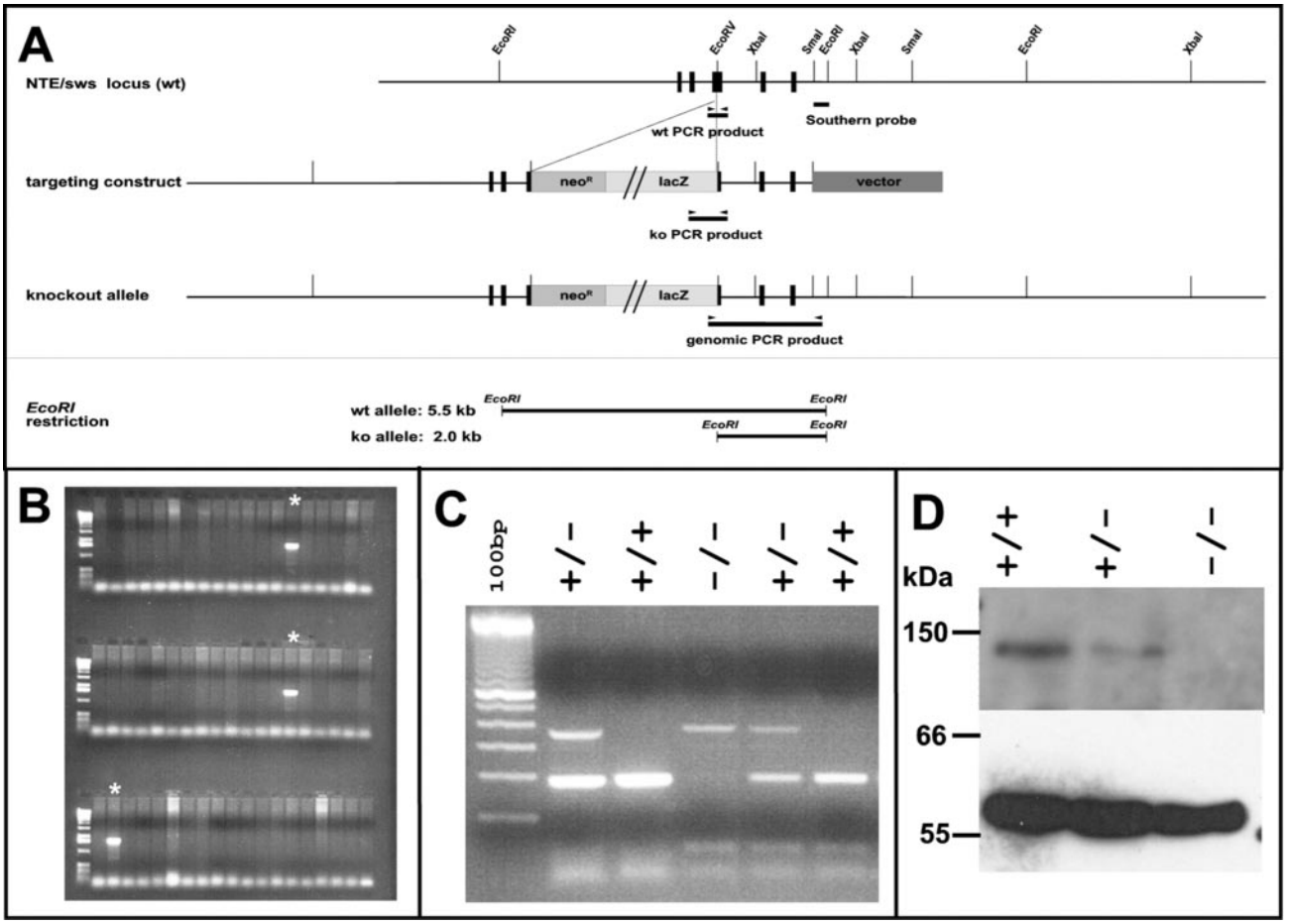

FIG. 1. NTE targeting vector and genotyping of mutant mice. (A) Schematic representation of the partial NTE gene locus and the targeting construct. Boxes, exons and the probe used for Southern hybridization of the neomycin-resistant stem cell clones, which recognizes the 5.5-kb wild-type (wt) and 2-kb mutant *Eco*RI fragments; arrowheads, primers used for screening ES cell DNA by genomic PCR. ko, knockout. (B) Homologous recombination resulted in generation of a 1.8-kb fragment (asterisk). (C) PCR analysis of yolk sac DNA from embryos derived from heterozygous matings. The positions of primer pairs for amplification of the 190-bp wild-type and 380-bp mutant PCR fragments are shown in panel A. (D) Western blots of cell lysates from in vitro-cultured wild-type, heterozygous, and NTE-null embryos were probed with rabbit anti-mouse NTE serum. Equal protein loading is shown by antitubulin staining.

Briefly, ES cells were cultured on irradiated mouse embryonic fibroblasts in the presence of leukemia inhibitory factor (Gibco-BRL, Gaithersburg, Md.); selection with 400 μg of G418 (Gibco-BRL)/ml was started 24 h after transfection, and then 240 neomycin-resistant clones were picked, expanded, and analyzed by Southern blotting of genomic *Eco*RI-digested DNA. An external probe comprising a 0.6-kb *Eco*RI/*Sma*I fragment of the NTE gene (see Fig. 1A) was used to identify the 5.5-kb wild-type allele and the 2.0-kb mutated allele. In addition a genomic PCR was performed to screen for homologous recombination events. Here, one primer was chosen to be outside the targeting vector and the other was chosen to be within the β-gal-neo cassette to amplify a 1.8-kb genomic fragment (NTR 5′up: TCA ACA GAC CTT GCA TTC CTT TGG C; SWS genPCRrev: TGG TAC AGG TCA GCT GGC CTT TCA C).

Three different ES cell clones with the targeted NTE allele were thawed 3 days prior to injection, injected into C57BL/6 blastocysts, and then reimplanted into 2.5-day-pseudopregnant NMRI females. Male chimeras were backcrossed to C57BL/6 and to 129/Sv mice, and heterozygous offspring were crossed to produce homozygous mutant offspring. The genotypes of these mice were assessed by PCR analysis using primers mSWS sense2 (ACC CTG GAC ATG TTC TAG CCA AAG) and mSWS anti1 (CTA GGG GAT GCT GTC TGA GGT C) to detect a 190-bp band for the wild-type allele and additional primer PGK polyA down (CTG CTC TTT ACT GAA GGC TCT TT) producing, together with mSWS anti-1, a 370-bp fragment for the mutant allele (see Fig. 1A).

Embryo cell culture for in vitro analysis. Embryos were dissected from maternal tissue and yolk sac at E8.0. Yolk sac DNA was isolated and used for genotyping. After being washed in PBS and ES cell medium, embryos were mechanically dissociated and cultured in fibronectin (5 μg/ml)-coated 24-well dishes with ES cell medium without leukemia inhibitory factor (50% was conditioned on feeder cells). Medium was changed after 4 days.

NTE expression: Northern and Western blotting and esterase assay. Northern blot analyses were performed using the same cDNA probe used for screening the genomic library. The randomly labeled fragment was hybridized with commercially available Northern blots (Seegene) by standard procedures (24). Expression of NTE protein in cultured cells from E8 embryos was determined by Western blotting. Approximately equal numbers of cells from wild-type, heterozygous, and NTE-null embryos were harvested and solubilized in sodium dodecyl sulfate (SDS) sample buffer. Polypeptides were resolved by SDS–7.5% polyacrylamide gel electrophoresis and electroblotted onto nitrocellulose. Blots were probed with a rabbit antiserum raised against a keyhole limpet hemocyanin conjugate with a synthetic peptide (CLPNQDDQGPRLEHPS) corresponding to the carboxyl terminus of mouse NTE. Equal loading of the samples was assessed by probing blots with a monoclonal antibody (clone B5-1-2) against tubulin (Sigma). NTE activity in tissue homogenates was measured by colorimetric assay of the hydrolysis of artificial substrate phenyl valerate as described previously (15).

Histology and TUNEL assay. After cervical dislocation of pregnant mice the decidual swellings were fixed in 4% paraformaldehyde–PBS overnight at 4°C and then dehydrated and embedded in paraffin. Five-micrometer-thick sections were made with a microtome and stained with hematoxylin and eosin. For analysis of

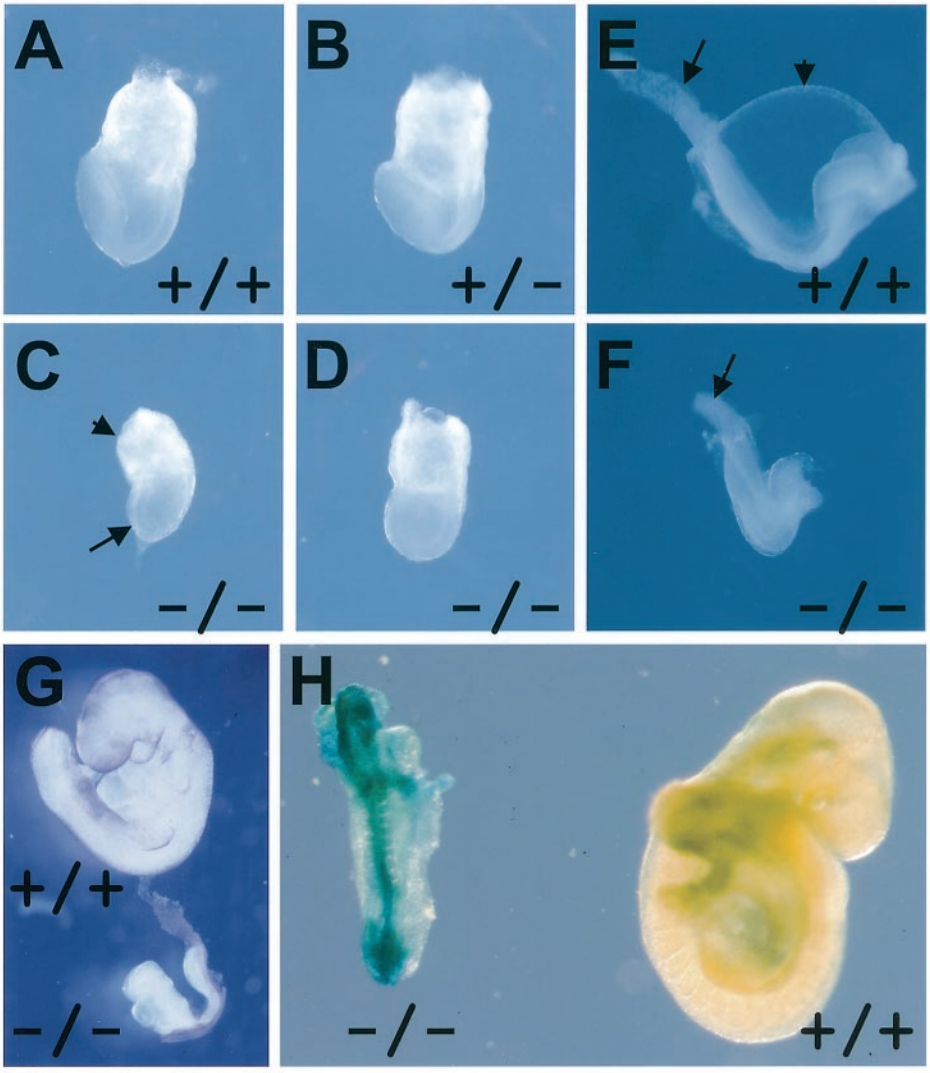

FIG. 2. NTE mutant embryos reveal growth retardation. (A to D) Embryos at E7. NTE mutants (C and D) are already slightly growth retarded at E7 compared to wild-type (A) and heterozygous (B) embryos from the same litter. Nevertheless, mutant embryos develop with embryonic (arrow) and extraembryonic (arrowhead) ectoderms. (E and F) At E8 growth retardation of the NTE knockout embryos (F) becomes more evident in comparison with a wild-type embryo (E). The allantois (arrows) and amnion (arrowheads) of the wild-type embryo are shown. (G) At E9 the developmental retardation becomes more obvious. (H) LacZ staining of a wild-type and NTE-heterozygous embryos at E9. LacZ is expressed throughout the heterozygous embryo, including head structures, neural tissue, somites, and tail bud, whereas no staining is present in the wild-type embryo. Panels A to D have the same magnification, as do panels E and F.

programmed cell death, the sections were stained based on reactivity determined by terminal deoxynucleotidyltransferase-mediated dUTP-biotin nick end labeling (TUNEL) using the Apop Teg in situ apoptosis detection kit (Oncor) according to the manufacturer's instructions (9).

BrdU labeling and immunohistochemistry. Timed pregnant mice from heterozygous matings were injected intraperitoneally at E8.5 and E9.5 with 5-bromo-2-deoxyuridine (BrdU; Sigma) at a dose of 50 μg/g of body weight. Pregnant mice were sacrificed 1.5 h after injection, and the uteri were removed. Decidual swellings were fixed in 4% paraformaldehyde at 4°C overnight and dehydrated, and then paraffin-embedded sections were processed for immunohistochemistry. For BrdU labeling, sections were pretreated with 2 N HCl for 30 min and incubated with an anti-BrdU mouse monoclonal antibody (Roche) at a dilution of 1:1,000 for 1 h at 37°C before a 30-min incubation with a horseradish peroxidase-conjugated anti-mouse secondary antibody (DAKO). Finally, sections were incubated with diaminobenzidine to detect nuclear staining. In parallel, the proliferation-associated antigen Ki67 was stained with a 1:750 dilution of an anti-Ki67 rabbit polyclonal antibody (Novocastra, Newcastle, United Kingdom) after sections were pretreated by being boiled three times in citrate buffer (pH 7.4) in a microwave. An ABC staining procedure (ABC Vector kit; Vector) was performed according to the manufacturer's instructions.

To determine apoptotic cell death, in addition to TUNEL staining, caspase 3 activity was detected by immunohistochemistry using an antibody that specifically interacts with the cleaved activated fragment of caspase 3. Immunohistochemistry was performed after permeabilization of the cells with 0.2% Triton X-100, boiling in 0.01 M citrate buffer in a microwave, and blocking in 5% goat serum–0.1% Tween in PBS containing a 1:200 dilution of the polyclonal antibody against cleaved caspase 3 (New England Biolabs). Detection by indirect immunoperoxidase staining was done with a Vectastain ABC kit (Vector).

In situ hybridization, whole-mount in situ hybridization, and LacZ staining. In situ hybridization of ^{33}P-labeled cRNA probes to paraffin-embedded tissue sections was described in detail previously (21). Two parallel tissue sections were mounted on each slide, and both antisense and, as a control, sense RNA probes were reacted to these sections under identical conditions. Probes detecting giant cells (expressing placental lactogen [Pl-1]) (3), spongiotrophoblast cells (expressing 4311) (19), and cells of the ectoplacental cone and cytotrophoblast cells (expressing Mash2) (12) were used to discriminate the different placental layers.

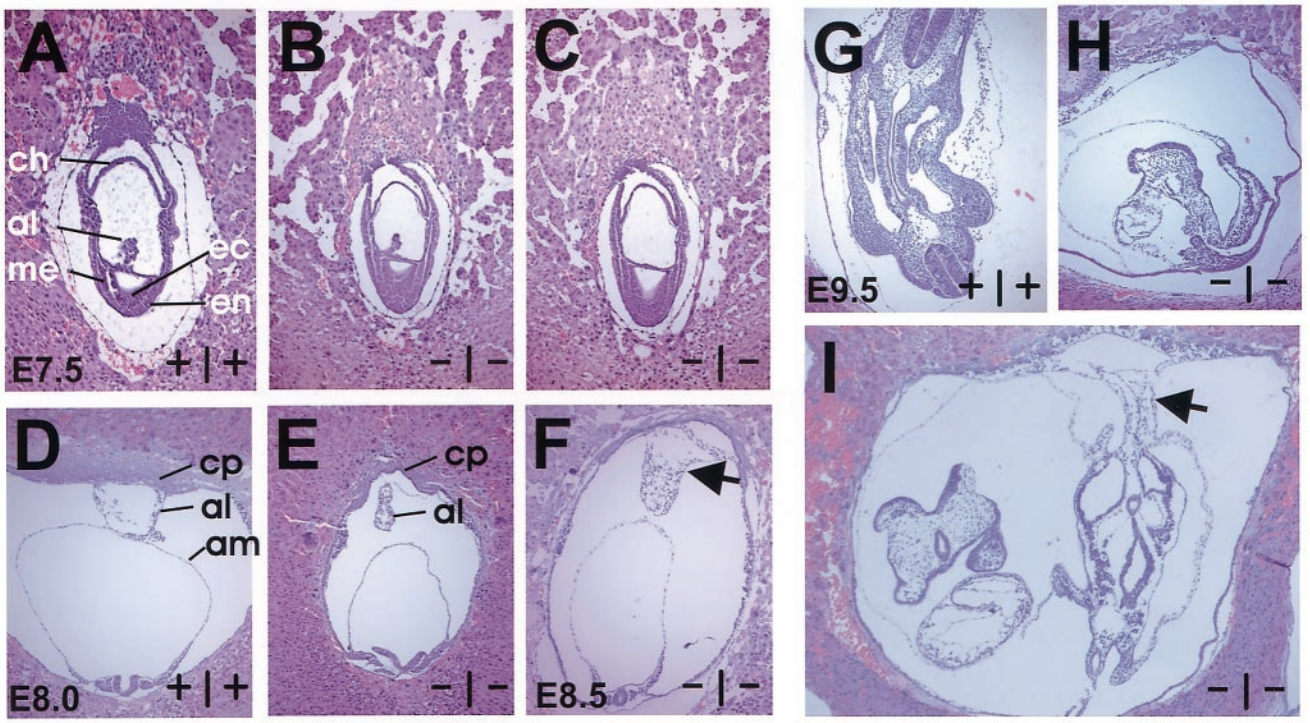

FIG. 3. Histological analyses of wild-type and NTE mutant embryos at E7.5 to E9.5. (A to C) Sagittal sections through E7.5 wild-type (A) and NTE mutant (B and C) embryos prove the formation of three germ layers, the allantois, and a thinner chorion in NTE-null embryos. (D to F) Chorioallantoic fusion occurs at E8 in wild-type embryos (D), whereas in NTE-null embryos fusion is delayed (E) and occurs at E8.5 (F; arrow). (G and H) Strong growth retardation at E9.5 can be seen by comparing histological sections of wild-type (G) and mutant (H) embryos. (I) Chorioallantoic fusion of E9.5 NTE-deficient mice. Note nucleated red blood cells in vessels of the allantois, indicating a functional connection with the chorion (arrow). al, allantois; am, amnion; ch, chorion; cp, chorionic plate; ec, ectoderm; en, endoderm; me, mesoderm. Panels A to C have the same magnification, as do panels D to F and panels G and H.

For LacZ staining, embryos were fixed in 2.5% glutaraldehyde–0.1 M PIPES (piperazine-*N*,*N*′-bis[2-ethanesulfonic acid]; pH 6.9)–2 mM $MgCl_2$–5 mM EGTA for 20 min before being washed in the same buffer without glutaraldehyde. After a short incubation for 5 min in PBS–0.02% NP-40–0.01% sodium deoxycholate to enhance penetration of the tissue, embryos were stained in 1 mg of X-Gal (5-bromo-4-chloro-3-indolyl-β-D-galactopyranoside)–1 mM $K_3[Fe(CN)_6]$–10 mM $K_4[Fe(CN)_6]$–2 mM $MgCl_2$/ml in PBS for several days.

RESULTS

Targeted disruption of the NTE allele in mice. To disrupt the NTE gene an IRES-β-gal-neo selection cassette was inserted into a central exon at the codon for amino acid 397 of the 1,327-residue murine NTE protein. By analogy to the three different mutant *Drosophila* strains which exhibit nonsense mutations at position ~365 or missense mutations at later positions of the cDNA, all resulting in nonfunctional SWS proteins (17; D. Kretzschmar, unpublished data), we expected that this insertion would result in a loss-of-function mutation in the NTE gene. The targeting vector had an overall homology with 5.5 kb of genomic sequence at the 5′ end and 1.8 kb at the 3′ end (Fig. 1A). The targeting vector was electroporated into R1 ES cells, and six homologous recombinants out of 240 G418-resistant clones were identified. Southern blot analysis of these clones revealed the presence of the 2.0-kb knockout fragment in addition to the 5.5-kb wild-type fragment after hybridization with an external genomic probe (data not shown). Homologous recombination was also shown by genomic PCR using primers within the selection cassette and outside of the targeting vector (Fig. 1B).

To generate mice harboring the targeted NTE allele, three ES cell clones were injected into C57BL/6 blastocysts, which gave rise to several chimeras. Chimeras from two independent ES cell clones transmitted the mutated allele to their offspring when crossed to C57BL/6 and 129/Sv females. No phenotypic differences between animals derived from the two independent clones were observed. Heterozygous mice of both sexes were healthy and fertile, and no overt phenotype was observed. Inactivation of NTE was confirmed by assay of its esterase activity in tissue homogenates. Activity in brain and kidney (223 ± 22 and 1,467 ± 133 nmol/min/mg of protein, respectively) of heterozygotes was 50% that for the wild type (451 ± 63 and 2,880 ± 319 nmol/min/mg of protein, respectively), suggesting equal expression of both alleles in wild-type animals.

Lack of NTE results in retarded growth and development and subsequent death during early gestation. Heterozygous mice were intercrossed to produce NTE homozygous mutant ($NTE^{-/-}$) offspring. Among 231 live-born progeny, no viable homozygous mutant offspring were identified, whereas 136 (59%) heterozygous and 95 (41%) wild-type offspring were recovered, indicating that homozygosity for the NTE mutation is embryonically lethal. To determine the time point of embryonic lethality and to characterize the morphological phenotype

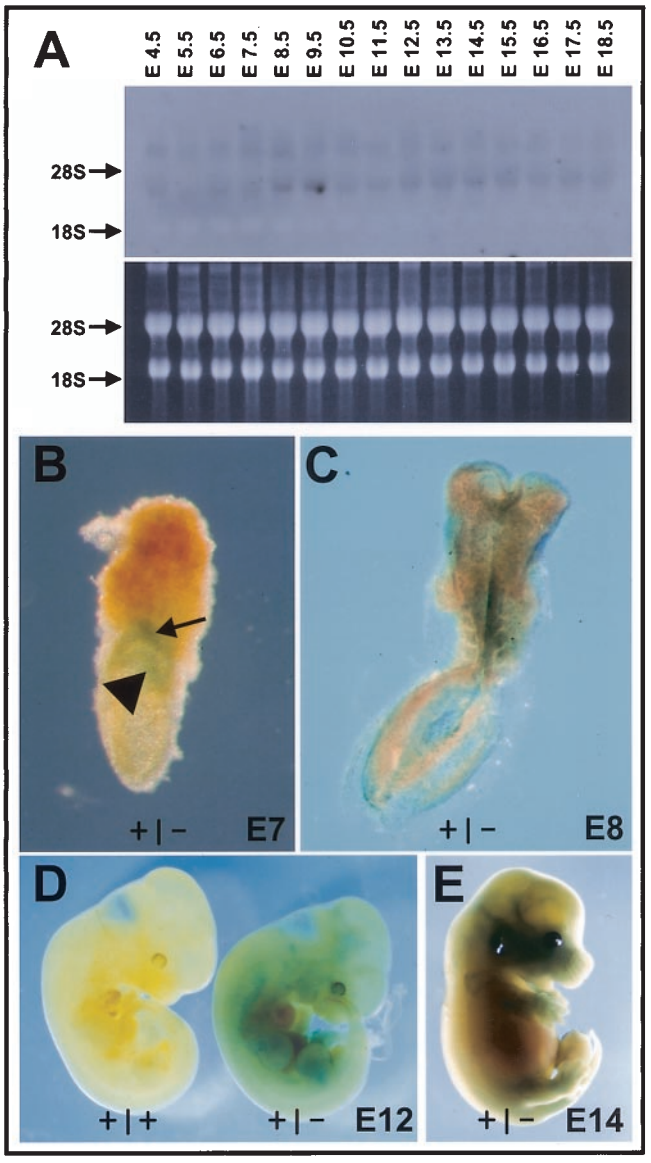

FIG. 4. Expression of NTE during embryonic development and in adult tissues. (A) Northern blot from total embryos between E4.5 and E18.5 reveals two transcripts of about 4.4 and 9 kb at all different time points examined. (B to E) LacZ staining of heterozygous embryos from E7 (B), E8 (C), E12 (D), and E14 (E) shows NTE expression in the extraembryonic ectoderm of the chorion (arrowhead) and ectoplacental cone (arrow) at E7; expression is visible in almost all tissues of the embryo at later stages. A wild-type embryo at E12 (D) lacks any LacZ staining and served as a control for staining specificity.

of mutant embryos, different stages of gestation were analyzed for the presence of NTE$^{-/-}$ offspring. The genotypes of the dissected embryos were determined by performing PCR of genomic DNA obtained from the yolk sacs of each embryo (Fig. 1C). In parallel, to demonstrate that gene targeting results in a protein-null mutation, we analyzed in vitro-cultured cells of E8 embryos by Western blotting using an antiserum against the carboxyl terminus of NTE; this confirmed the reduction of NTE protein levels in cells from heterozygotes and its elimination from NTE-null embryos (Fig. 1D).

NTE$^{-/-}$ embryos were detected from E7.5 to E9.5. Even at E7.5, null mutant embryos were slightly smaller than the wild type and heterozygotes (Fig. 2A to D). This retardation was more obvious by E8.5 and E9.5, and an increased number of resorbed and empty conceptuses were observed. E8.5 NTE-deficient embryos had only 2 to 6 somites and were half the size of their wild-type or heterozygous littermates, which had 8 to 12 somites (Fig. 2E and F). Surviving NTE mutants at E9.5 could be easily distinguished from their littermates by their much smaller size, pale color, enlarged pericardium, and incomplete process of turning. Due to growth retardation the cranial neural plate was still not fused (Fig. 2G and H). Mutant embryos could occasionally be isolated at E10.5 but were not alive and often already in the process of resorption.

Histological sections revealed that E7.5 NTE mutant embryos are in the process of gastrulation and have formed all three germ layers and apparently normal extraembryonic membranes (Fig. 3A to C). At E8.0 the whole embryonic cavity of the decidual swelling is smaller in mutants than in wild-type or heterozygous embryos (Fig. 3D). Chorioallantoic fusion is slightly delayed in NTE mutants and occurs at around E8.5 (Fig. 3F). Sections of E9.5 knockout embryos demonstrate the strong developmental delay, although an apparently functional chorioallantoic fusion with vessels containing embryonic blood cells has been formed (Fig. 3G to I).

NTE is widely expressed in early development. Since the early embryonically lethal phenotype indicates an indispensable function for NTE, we analyzed the expression of NTE during fetal development. As early as E4.5, two NTE transcripts (4.4 and ~9 kb) could be detected by Northern blotting, and their expression appeared to increase to a maximum at E8.5 to E9.5 and decline slightly thereafter (Fig. 4A). From E7.5 to E15.5 expression of NTE was detected by LacZ staining of whole-mount NTE-heterozygous embryos (Fig. 4B to E). At E7.5, expression was most intense in the extraembryonic ectoderm of the chorion and the ectoplacental cone (Fig. 4B). From E8.5 onward, NTE expression was detected in many tissues throughout the embryo (Fig. 4C to E).

Analysis of cell proliferation and apoptotic cell death in NTE mutant mice. Since NTE expression was detected in all embryonic developmental stages, we first analyzed the proliferation of NTE mutant blastocysts in vitro. LacZ staining of in vitro-cultivated NTE-heterozygous blastocysts revealed positive cells within the inner cell mass and also in trophoectodermal cells. Nevertheless, NTE-null blastocysts showed a normal phenotype, indicating that the NTE mutation does not affect preimplantational growth. In addition, after 5 days in culture the inner cell mass and the trophoblast cells of NTE-deficient embryos showed the same outgrowth as wild-type blastocysts (data not shown). These observations strongly suggest that at this early stage of development NTE function is not required for proliferation and cell survival.

To analyze directly the effect of NTE mutation on cellular proliferation at later embryonal stages, we measured the incorporation of BrdU into DNA during S phase of the cell cycle. At E8.5 and E9.5 pregnant female mice were injected with BrdU and whole litters were dissected 1.5 h later. BrdU incorporation was detected by immunohistochemical staining. Although positive nuclear staining was clearly detected in normal

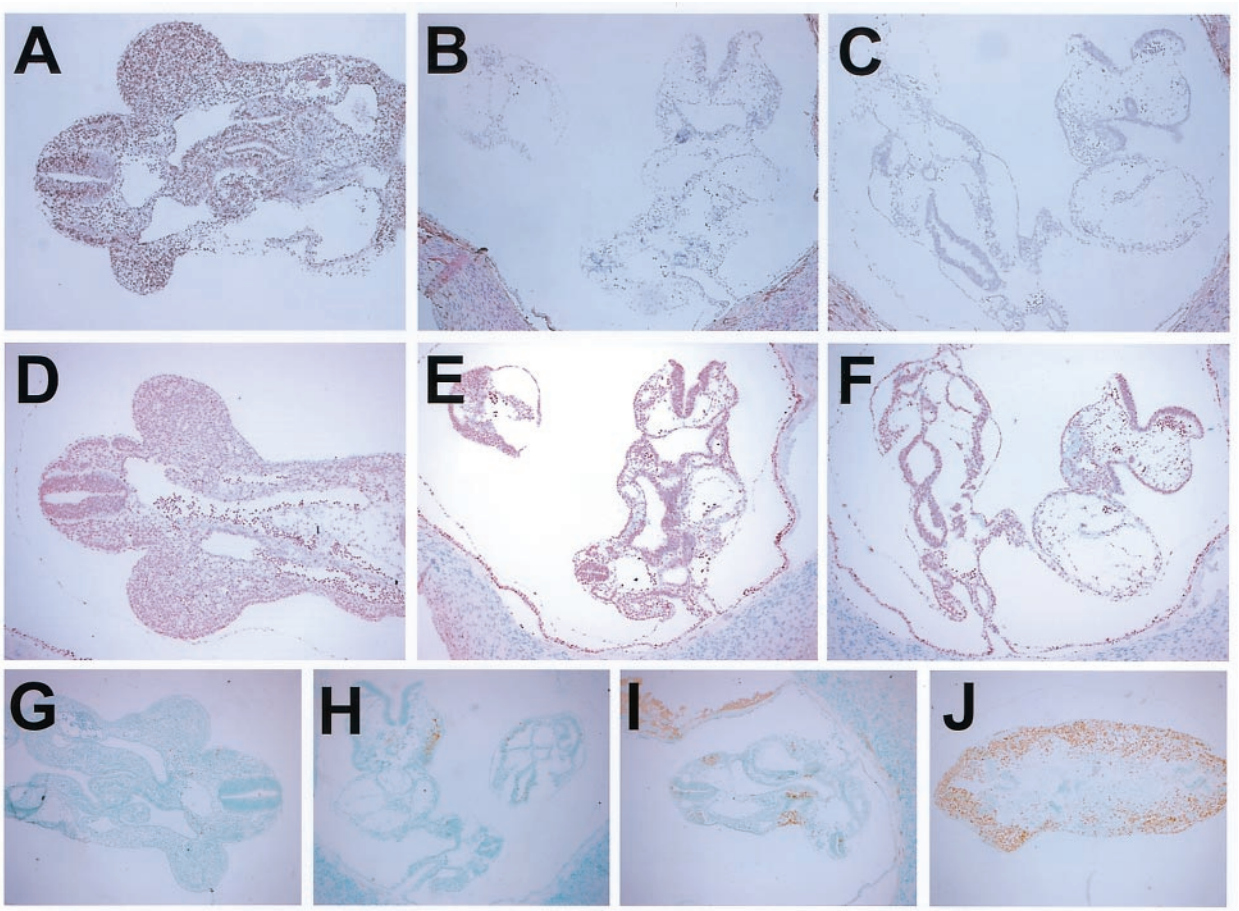

FIG. 5. Cell proliferation and cell death in NTE mutant embryos. BrdU labeling experiments reveal no labeled cells in NTE-deficient embryos (B and C), whereas wild-type embryos reveal strong proliferation throughout the embryo (A). However, Ki67 staining indicates that cell proliferation in knockout mice (E and F) is indistinguishable from that in normal embryos (D). (G to J) TUNEL staining of E9.5 (G to I) and E10.5 (J) mouse embryos of wild-type (G) and NTE-deficient mice (H to J) indicates massive cell death already at E9.5 in various regions of the embryo in comparison to only a few positive cells in the wild-type embryo (G). The same magnification was used for all panels.

embryos, NTE mutant embryos had not incorporated BrdU into their DNA, suggesting either a defect in cellular proliferation or defects in placentation or yolk sac circulation resulting in greatly reduced availability of BrdU to the embryo (Fig. 5A to C). To distinguish between these possibilities, we measured cellular proliferation in NTE mutant embryos by a second experimental approach. Using an antibody against the nuclear antigen Ki67, which is present in the nuclei of all proliferating cells (25), immunohistochemical staining showed unaffected cellular proliferation in mutant embryos, which was not significantly different from that in the wild-type littermates (Fig. 5D to F).

We next analyzed cell death in NTE mutant embryos by TUNEL staining of E8.5 and E9.5 embryo sections. TUNEL-positive cells were detected at E9.5 in the whole embryo both in the head and the trunk regions (Fig. 5G to J). Cell death affected tissues derived from all three germ layers, including neural tissues, somites, and endodermal structures. Since TUNEL staining cannot discriminate between actively dying apoptotic cells and necrotic cells, we performed immunohistochemistry with an antibody that recognizes the activated cleaved form of caspase 3. These stainings clearly indicated that a large number of cells in many different tissues die by apoptosis (data not shown).

Since NTE-deficient embryos do not suffer from impaired cellular proliferation, we next addressed the question of whether the observed cell death is due to a lack of an essential cellular function of NTE or to extraembryonic defects. Therefore E8 embryo cells were disaggregated and seeded on fibronectin-coated dishes (see Materials and Methods). Although NTE mutant embryos are significantly smaller at this stage of development, and therefore fewer cells and colonies survived after 1 week of culture, their cells could be cultivated for more than 1 week. The colonies gave rise to different cell types with different cell morphologies (Fig. 6A and B). From three more properly developed NTE mutants, we obtained highly differentiated cells, such as beating cardiac myocytes and cells resembling neurons with long branched neurite-like processes (Fig. 6C). Taken together, these data demonstrate that NTE mutant embryos do not exhibit a general defect in cellular proliferation and that a number of different cells can survive in the absence of NTE activity.

Lack of NTE causes defects in extraembryonic tissues. First indications of a defect in placenta formation were derived from

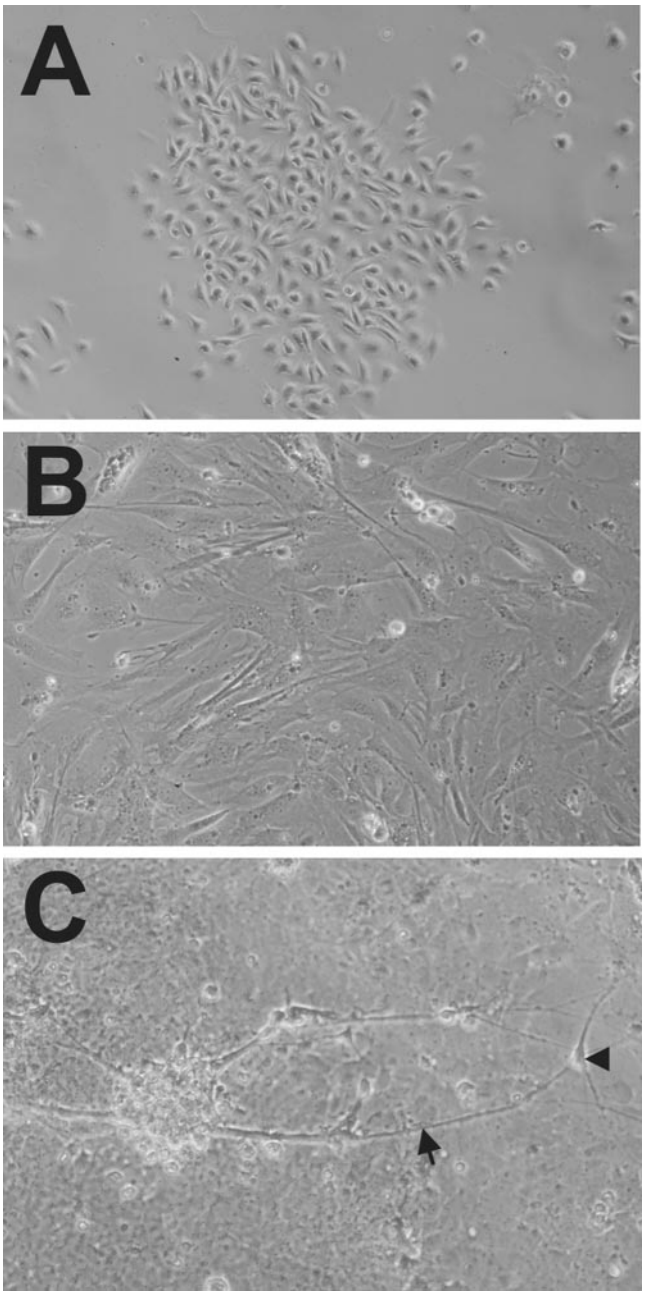

FIG. 6. NTE-deficient cells survive in vitro. Isolated cells from E8 NTE-null embryos survive several days in culture and differentiate into a number of different cell types (A and B), including cells (C) with long (arrow) and branched (arrowhead) neurite-like processes.

inspection of the much smaller decidual swellings of NTE$^{-/-}$ embryos at around E9, since during normal development the growing placenta induces decidual tissue formation. At E7.5, the morphology, number, and distribution of trophoblastic giant cells in NTE-deficient embryos appeared normal but the condensed packed cells of the ectoplacental cone were almost absent and the extraembryonic ectodermal sheet of the chorion itself seemed to be thinner than in wild-type embryos (Fig. 7A to D). Half a day later, in the mutant conceptus, a thin curved chorionic plate had formed and the ectoplacental cone was clearly smaller than normal (Fig. 7E to H). At E8.5, fusion of the chorion and allantois had occurred in mutants (Fig. 7J), about half a day later than in the wild type (Fig. 7E and G). A higher magnification of these structures revealed that the chorionic plate and the ectoplacental cone were less densely packed in NTE mutant conceptuses, and the cell or nucleus seems to be bigger in mutant ectoplacental cones. At E9.5, the wild-type placenta had acquired the typical three-layer appearance, with the labyrinth layer above the chorion/allantois forming the inner layer, the spongiotrophoblast forming the middle layer, and the giant cells forming the outer layer and the interface with the maternal deciduae. In NTE-null mutants the labyrinth layer failed to form: although the chorionic trophoblast differentiation and morphogenesis had begun through interdigitation of the allantoic mesoderm and underlying fetal vessels with chorionic plate trophoblast cells to form simple branches (Fig. 7M and N), these branches failed to elongate and bifurcate, but rather collapsed at E10. Maternal blood sinuses were completely absent in mutant placentas (Fig. 7O and P). In addition to the obvious failure in labyrinth formation, the number of trophoblast giant cells was decreased by E8.5 and more obviously so at later stages, when only a few giant cells were distributed on top of the invading ectoplacental cone (Fig. 7I and P). Taken together, the primitive capillary network in NTE-null mutants is obviously not sufficient for proper exchange of nutrients and gases between the maternal blood circulation and the developing embryo.

To further characterize the placental defect, we analyzed the expression of several trophoblast markers (Fig. 8). At E7.5 to E8.5, trophoblast giant cells expressing Pl-1 (3) were present in comparable numbers in wild-type and mutant placentas. However, at E9.5, only a few scattered giant cells were found in mutant placentas compared to a continuous layer of Pl-1-expressing giant cells surrounding the embryonic cavity in wild-type placentas. The marker Mash2 was used to label the ectoplacental cone, the chorion, and their derivatives, the syncytiotrophoblast cells of the labyrinth, in the placenta (12). In mutant placentas, Mash2 labeled cells in the curved chorionic plate at E8 and in the reduced ectoplacental cone at E8.5 but almost no Mash2 signal was detected at E9.5, indicating that the chorionic trophoblast cells had failed to differentiate into syncytiotrophoblast cells of the labyrinth. In contrast, ectoplacental cone cells of E9.5 mutant placentas had obviously differentiated into spongiotrophoblast cells, which are detected by the marker 4311 (19) (Fig. 8). These results indicate that inactivation of NTE affects not only the chorion, from which the labyrinth layer of the placenta is formed, but also the ectoplacental cone and the production or survival of secondary giant cells.

Finally, we analyzed cell proliferation and death in the placenta. TUNEL staining from E8 onward revealed significantly more dying cells in null mutant than wild-type placentas, suggesting that NTE is essential for the survival of ectoplacental cone cells (Fig. 9A to D). In parallel, cell proliferation was studied by using BrdU incorporation and immunohistochemistry against Ki67. Both methods showed that in mutant placentas proliferation was restricted to the chorionic plate and the cells of the ectoplacental cone showed less nuclear staining. However, at E9.5 trophoblast stem cells from the chorion still

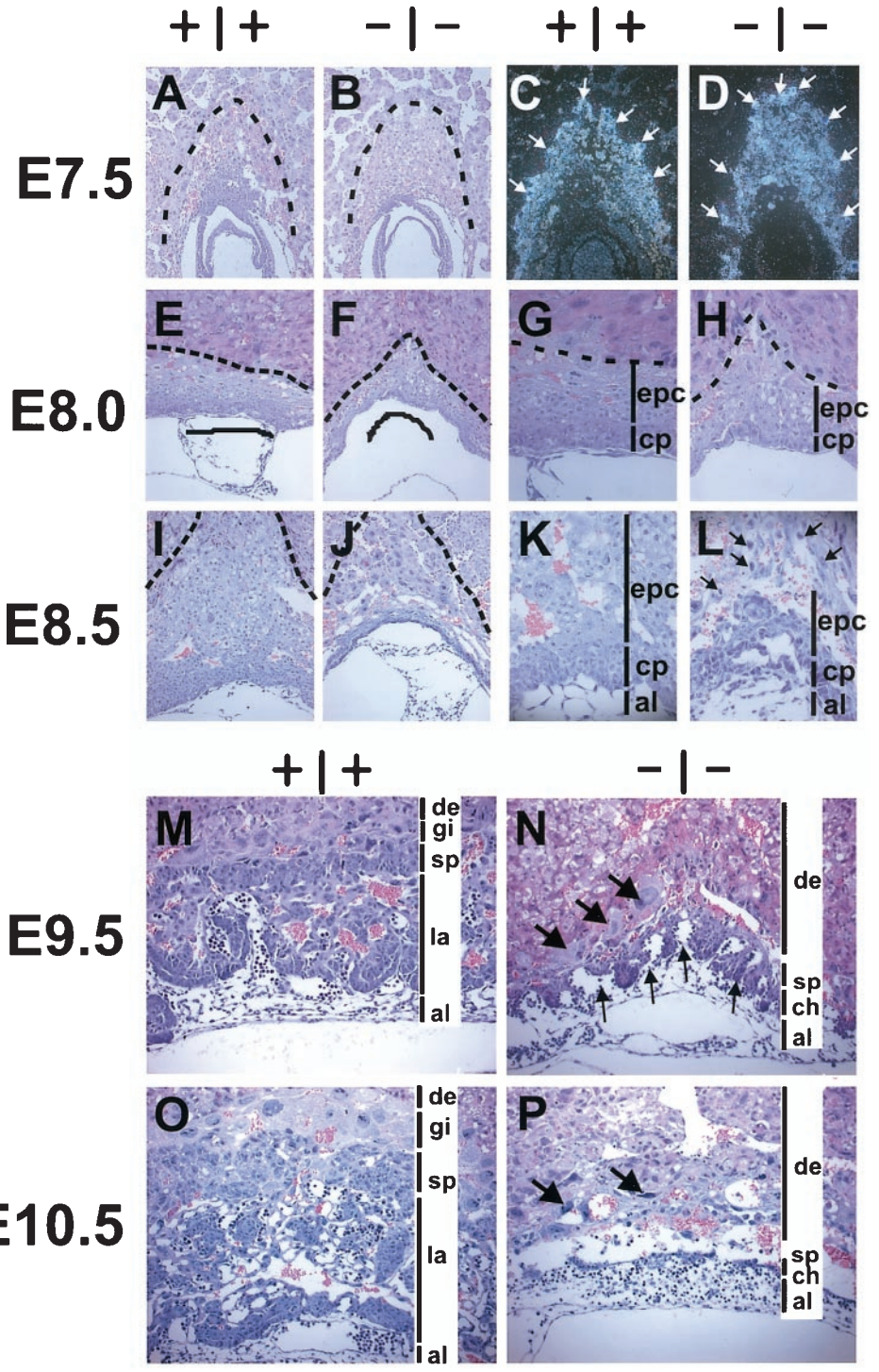

FIG. 7. Defects in placental development in NTE mutants. Histology of the placenta in NTE mutant conceptuses. (A to D) Histological sections of wild-type and NTE mutant placentas at E7.5. (C and D) In situ hybridizations with the giant cell marker Pl-1. Arrows, giant cells. Note that the compact cells of the ectoplacental cone are almost absent in NTE mutants and that the chorion is much thinner than it is in wild-type extraembryonic tissue. At E8.0 the chorionic plate is curved in NTE mutant placentas (F), compared to the flat chorionic plate of wild-type placentas (E) (bar and curve). (G and H) Higher-magnification version of panels E and F showing the smaller ectoplacental cone (epc) and the thinner chorionic plate (cp) of mutant placentas. (I to L) At E8.5 defects in placental development become more evident. The sizes of the ectoplacental cone and the chorion are strongly reduced, and fewer giant cells (L; arrows) are detectable in mutants. In addition, the nuclei and cells of the ectoplacental cone seem to be bigger in NTE-deficient placentas. Panels K and L are higher-magnification versions of panels I and J, respectively). (M to P) Placentas at developmental stages E9.5 and E10.5. Locations of the allantois (al), labyrinth (la), spongiotrophoblast layer (sp), giant cells (gi), and maternal deciduae (de) are indicated. Big arrows (N and P), giant cells in mutant placentas; small arrows (N), folds within the chorion, where primitive embryonic vessels start to form. At E10.5 the mutant placenta is totally collapsed. Only a few giant cells (arrow) and a thin layer of chorion and spongiotrophoblast cells remain (P). Compared pictures were taken at the same magnification. Dotted lines mark the interface between trophoblast giant cells and decidua.

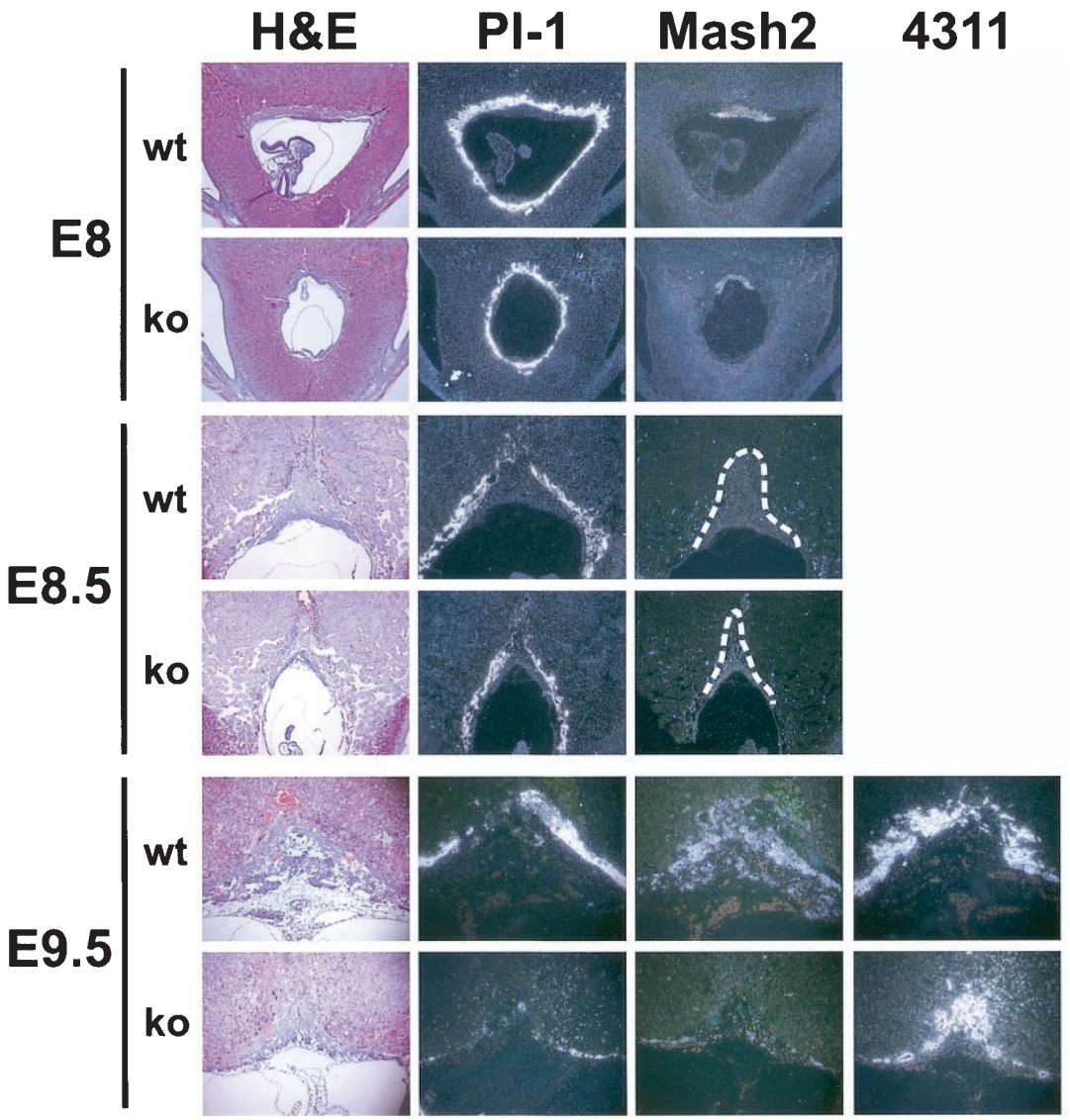

FIG. 8. Trophoblast marker analysis of NTE mutants at E8.0, E8.5, and E9.5. Serial sections of wild-type (wt) and mutant (knockout [ko]) conceptuses were probed with antisense riboprobes for Pl-1, Mash2, and 4311. Pl-1 is expressed in trophoblast giant cells; Mash2 is expressed in the chorionic plate at E8.0, the ectoplacental cone at E8.5, and the labyrinth and spongiotrophoblast cells at E9.5; and 4311 is expressed in the spongiotrophoblast layer of E9.5 placentas. Note that at E9.5 almost no giant cells are labeled and no labyrinth has formed in NTE mutants, whereas spongiotrophoblast cells are present in NTE-deficient placentas. Strikingly these cells are negative for Mash2. All pictures were taken with the same magnification. Dotted lines indicate the size and shape of the ectoplacental cone. H&E, hematoxylin and eosin.

proliferate and syncytiotrophoblast precursor cells form around the developing fetal vessels and invade toward the maternal blood sinuses (Fig. 9E to J).

NTE is required for vasculogenesis. The extraembryonic yolk sac is the first site of hematopoiesis in the mouse embryo, and, upon fusion of the yolk sac and embryonic vasculatures, it is the primary source of blood cells for the embryo. The yolk sac is composed of mesodermal and visceral endodermal cell layers, and the yolk sac mesodermal cells proliferate and differentiate into blood islands. Individual blood islands fuse by vasculogenesis, forming a vascular network containing primitive, nucleated red blood cells. NTE mutants at early phases of yolk sac development (E8.0 and E8.5) appeared completely normal. Blood islands were formed and endothelial cells lined the newly formed blood vessels (Fig. 10A to D). However, at E9.5, vasculogenesis was clearly blocked in NTE-deficient yolk sacs: mesodermal and endodermal cell layers had collapsed, and no vascular network had been established (Fig. 10E and F).

Vasculogenesis also occurs within the embryo at E9.5, forming, for example, the dorsal aortae. Although vessels within mutant embryos were lined by endothelial cells, many of these vessels were heavily dilated and severe hemorrhages were found in the head (Fig. 10G). A paired dorsal aorta was observed in horizontal sections of some NTE-null embryos, but other dilated vessels filled with nucleated embryonic blood

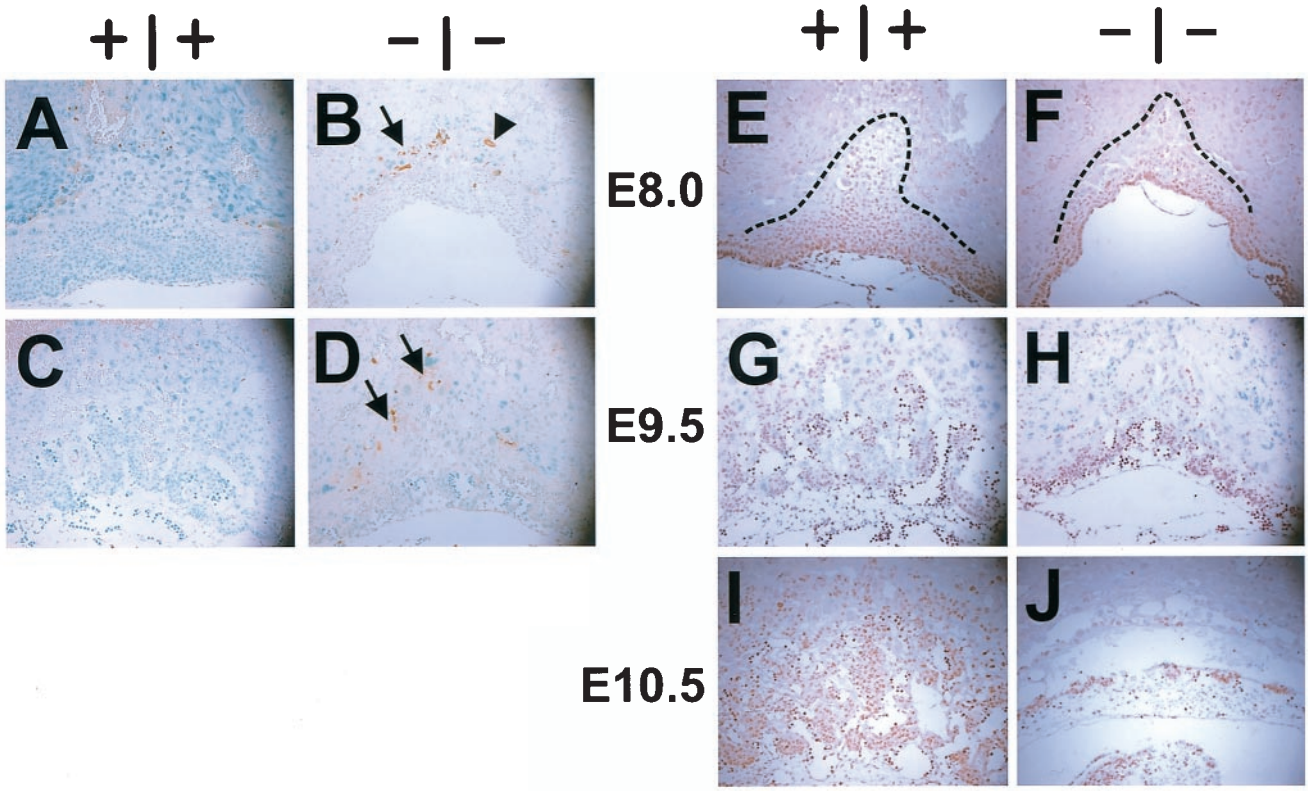

FIG. 9. Apoptosis and cell proliferation in NTE-deficient placentas. There is significantly higher apoptotic cell death in the placentas of NTE mutants. (A to D) TUNEL staining reveals apoptosis already at E8.0 within the ectoplacental cone (arrows) and giant cells (arrowhead) of NTE mutants, whereas only a few apoptotic cells are stained at the interface between the ectoplacental cones and deciduae of wild-type placentas. There are more apoptotic cells in the ectoplacental cone of NTE-null placentas. Proliferation is not impaired in the placentas of NTE mutants but is mainly restricted to the chorionic plate at E8.0 (F) and to the chorionic stem cells at E9.5 (H). Even at E10.5, the remaining chorionic stem cells still proliferate (J). Proliferating cells were detected by anti-Ki67 immunohistochemistry. Dotted lines indicate the border between ectoplacental cone and giant cells.

cells were also present (Fig. 10H). Thus, embryonic vasculogenesis appears to require NTE activity.

The genetic background of the mice had a marked influence on the onset of embryonic death. Most of the experiments reported here were on conceptuses engendered on a mixed Sv129-C57BL/6 background. However, 10 backcrosses to a C57BL/6 background exacerbated the developmental defects so that NTE-null embryos often died by E8 or E8.5, about 1.5 days earlier than those on the mixed background. Since placenta formation is not essential for embryo survival at E8.5, vascular defects are probably the major cause of embryonic death in NTE-null mutants on the C57BL/6 background.

DISCUSSION

We show here that NTE-null mice die by midgestation. As our study neared completion, Winrow et al. reported the same observation but did not investigate the cause of embryonic lethality (29). Our present analysis reveals that NTE is required both for placenta formation and for vasculogenesis within the extraembryonic yolk sac and the embryo itself: failure of either of these critical processes would result in embryonic death.

NTE is expressed in cells of the inner cell mass and in trophoectodermal cells of the blastocyst but is not essential for cell survival and proliferation at this early developmental stage. Even at E8.5 and E9.5, cellular proliferation in NTE-null embryos is unimpaired, and cells isolated from these embryos at E8 survive and differentiate in vitro. By contrast, our data demonstrate that NTE is absolutely essential for proper placentation of the embryo. Although early steps of implantation occur normally in NTE-null conceptuses, by E8.0 and later the connection between the trophoblast and the decidua is impaired. This connection is essential for nutrition of the embryo before the development of the yolk sac. Although primary giant cells invade the maternal decidual tissue in NTE-null conceptuses, extraembryonic tissue of the ectoplacental cone revealed a significantly delayed and reduced invasion and proliferation capacity.

One consequence of this primitive ectoplacental cone might be a lower rate of giant cell generation from progenitors of the ectoplacental cone or spongiotrophoblast cells. Although spongiotrophoblasts expressing the marker 4311 are well represented in NTE-null placentas, another marker, Mash2, normally also expressed in spongiotrophoblasts and cells in the chorion, labyrinth, and ectoplacental cone, is no longer detectable at E9.5. Spongiotrophoblasts differentiate from the ectoplacental cone and harbor progenitors of secondary giant cells.

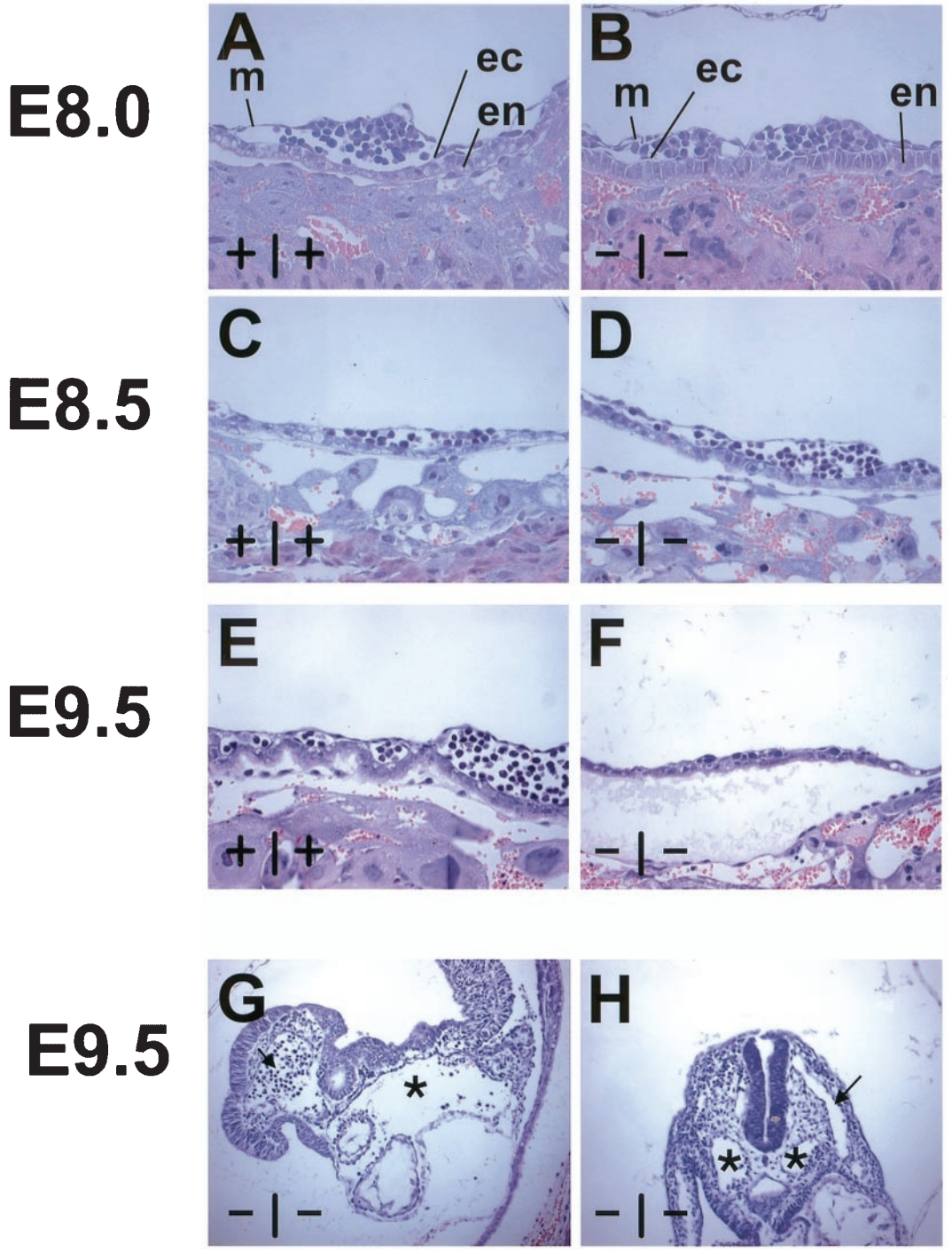

FIG. 10. Vascular defects in yolk sac and within the embryos of NTE mutants. (A to D) Vascularization of the yolk sac initially occurs normally. Blood islands are lined by endothelial cells (ec), the mesoderm (m), and the visceral endoderm (en). (E and F) Vascularization collapses at E9.5, when vasculogenesis occurs in wild-type yolk sacs. (G) Sagittal sections through an E9.5 NTE mutant embryo reveal severe hemorrhages in the head (arrow) or extremely dilated dorsal aortae (*). (H) In other embryos the paired dorsal aortae seemed to be less affected (*) but other blood vessels are dilated (arrow).

Mash2 inhibits giant cell formation and maintains proliferating trophoblasts, and thus Mash2-null mice have an increased number of giant cells (4, 7, 28). By contrast, formation of giant cells from the ectoplacental cone or spongiotrophoblast cells in NTE-null mice seems to be blocked, resulting in an only weakly anchored placental structure inside the decidua.

A number of critical steps during placental development are not affected in NTE-deficient mice, and these serve to distin-

guish this phenotype from those of several other loss-of-function mutants. NTE-null embryos attach to the yolk sac and, at first, a functional vitelloembryonic circulation occurs, with nucleated blood cells filling the vessels of the embryo. One common cause of midgestation embryonic lethality in mice is the failure of chorioallantoic fusion, resulting in a failure of placental development. However, NTE-null embryos differ from Vcam1- (vascular cell adhesion molecule 1) and α-4 integrin-deficient mutants (13, 18, 30) in that chorioallantoic attachment and fusion occur in the former, although this process is slightly delayed. Even the next essential step of placenta formation, the chorioallantoic branching, is initiated with the formation of simple villi at E9. These villi are formed by folds in the chorion trophoblast surface. Points at which folding occurs in the chorionic plate and at which evagination of the chorionic mesoderm is initiated are preceded by the expression of the transcription factor Gcm1 (glial cells missing 1) (1). Gcm1-expressing cells are confined to the tip of elongating branches, where trophoblast cells elongate and fuse to form the syncytiotrophoblast layer. In the absence of Gcm1, chorioallantoic branching fails to initiate, mutants arrest at the flat chorion stage, and chorionic trophoblast cells fail to differentiate into syncytiotrophoblasts (1, 26). Chorioallantoic branching is initiated in NTE-deficient mice, which differ in this respect from Gcm1-null mice, and very primitive branches are present at E9.5; furthermore, the chorionic stem cells lying between the sites where initial folding occurs proliferate rapidly. However, similar to the phenotype of Gcm1-null mice, further differentiation of syncytiotrophoblast cells failed in NTE mutants, resulting in the complete absence of the labyrinth. The observed phenotype correlates with the expression of NTE in the extraembryonic ectoderm of the chorion, the ectoplacental cone, and trophoblast giant cells. Obviously, NTE activity is essential during the differentiation of these cells, leading to a complete absence of the labyrinth, a reduced ectoplacental cone, and a giant cell defect.

In parallel, the epiblast develops normally and the formation of the definitive germ layers through gastrulation happens without delay in NTE-null embryos. The postgastrulation period involves a rapid increase in embryonic mass. NTE-deficient embryos exhibit at that time point enlarged pericardia and dilated blood vessels in the head and trunk regions. Although vasculogenesis is not impaired, an effective cardiovascular circulation is obviously not maintained, and, consequently, there is a reduction of cell proliferation and cell viability in NTE-null embryos. The well being of the embryo is critically dependent on the formation and maintenance of a functioning yolk sac circulation, which is initially well established in NTE mutants but is blocked when blood vessels are formed. The cessation of blood flow within the yolk sac plexus is followed by growth retardation and by swelling of the pericardium. Targeted mutagenesis in mice of a number of genes (the vascular endothelial growth factor, flk-1, and flt-1 genes) involved in blood vessel formation inside the embryo and also in the yolk sac reveals similar defects and leads to embryonic death at midgestation (2, 6, 8, 27). In particular, the phenotype of flt-1 knockout mice reveals some interesting conformity with NTE mutant embryos. flt-1-null mice form endothelial cells in both embryonic and extraembryonic regions, but these cells become assembled into abnormal vascular channels (8). In NTE mutant conceptuses, vascular defects found in the embryo proper and in the yolk sac would be lethal, independent of failure to form the chorioallantoic placenta.

The neurodegenerative phenotype of sws mutant flies (17) suggests that NTE may well have a role in vertebrate neural development and maintenance. The embryonic lethality in NTE knockout mice reported here and by Winrow et al. (29) indicate that investigation of NTE's potential neural function will require creation of conditional knockout mice and in vitro studies using RNA interference. Equally interesting will be the elucidation of the NTE-mediated process required for survival of both neurons in *Drosophila* brain and cells in the placenta. Finally, the phenotype of NTE-null mice implies that maternal exposure to neuropathic OP during early pregnancy could cause embryonic death.

ACKNOWLEDGMENTS

This work was supported by grants from the Deutsche Forschungsgemeinschaft to M.M. and R.B.

We thank D. I. Linzer (PL-1), J. Rossant (4311), and A. Joyner (Mash2) for kindly providing cDNA probes.

REFERENCES

1. **Anson-Cartwright, L., K. Dawson, S. J. Fisher, R. A. Lazzarini, and J. C. Cross.** 2000. The glial cells missing-1 protein is essential for branching morphogenesis in the chorioallantoic placenta. Nat. Genet. **25:**311–314.
2. **Carmeliet, P., V. Ferreira, G. Breier, S. Pollefeyt, L. Kieckens, M. Gertsenstein, M. Fahrig, A. Vandenhoeck, K. Harpal, C. Eberhardt, C. Declercq, J. Pawling, L. Moons, D. Collen, W. Risau, and A. Nagy.** 1996. Abnormal blood vessel development and lethality in embryos lacking a single VEGF allele. Nature **380:**435–439.
3. **Colosi, P., F. Talamantes, and D. I. Linzer.** 1987. Molecular cloning and expression of mouse placental lactogen I complementary deoxyribonucleic acid. Mol. Endocrinol. **1:**767–776.
4. **Cross, J. C., M. L. Flannery, M. A. Blanar, E. Steingrimsson, N. A. Jenkins, N. G. Copeland, W. J. Rutter, and Z. Werb.** 1995. Hxt encodes a basic helix-loop-helix transcription factor that regulates trophoblast cell development. Development **121:**2513–2523.
5. **Ehrich, M., and B. S. Jortner.** 2001. Organophosphorus-induced delayed neuropathy, p. 987–1012. *In* R. Krieger (ed.), Handbook of pesticide toxicology, 2nd ed. Academic Press, San Diego, Calif.
6. **Ferrara, N., K. Carver-Moore, H. Chen, M. Dowd, L. Lu, K. S. O'Shea, L. Powell-Braxton, K. J. Hillan, and M. W. Moore.** 1996. Heterozygous embryonic lethality induced by targeted inactivation of the VEGF gene. Nature **380:**439–442.
7. **Firulli, A. B., D. G. McFadden, Q. Lin, D. Srivatava, and E. N. Olson.** 1998. Heart and extra-embryonic mesodermal defects in mouse embryos lacking the bHLH transcription factor Hand1. Nat. Genet. **18:**266–270.
8. **Fong, G. H., J. Rossant, M. Gertsenstein, and M. L. Breitman.** 1995. Role of the Flt-1 receptor tyrosine kinase in regulating the assembly of vascular epithelium. Nature **376:**66–70.
9. **Gavrieli, Y., Y. Sherman, and S. A. Ben-Sasson.** 1992. Identification of programmed cell death in situ via specific labeling of nuclear DNA fragmentation. J. Cell Biol. **119:**493–501.
10. **Glynn, P., J. L. Holton, C. C. Nolan, D. J. Read, L. Brown, A. Hubbard, and J. B. Cavanagh.** 1998. Neuropathy target esterase: immunolocalisation to neuronal cell bodies and axons. Neuroscience **83:**295–302.
11. **Glynn, P.** 2000. Neural development and neurodegeneration: two faces of neuropathy target esterase. Prog. Neurobiol. **61:**61–74.
12. **Guillemot, F., A. Nagy, A. Auerbach, J. Rossant, and A. L. Joyner.** 1994. Essential role of Mash-2 in extraembryonic development. Nature **371:**333–336.
13. **Gurtner, G. C., V. Davis, H. Li, M. J. McCoy, A. Sharpe, and M. I. Cybulsky.** 1995. Targeted disruption of the murine VCAM1 gene: essential role of VCAM-1 in chorioallantoic fusion and placentation. Genes Dev. **9:**1–14.
14. **Johnson, M. K.** 1969. The delayed neurotoxic effect of some organophosphorus compounds: identification of the phosphorylation site as an esterase. Biochem. J. **114:**711–714.
15. **Johnson, M. K.** 1977. Improved assay of neurotoxic esterase for screening organophosphates for neurotoxic potential. Arch. Toxicol. **37:**113–115.
16. **Johnson, M. K.** 1982. The target site for initiation of delayed neurotoxicity by organophosphorus esters: biochemical studies and toxicological applications. Rev. Biochem. Toxicol. **4:**141–212.
17. **Kretzschmar, D., G. Hasan, S. Sharma, M. Heisenberg, and S. Benzer.** 1997.

The Swiss cheese mutant causes glial hyperwrapping and brain degeneration in *Drosophila*. J. Neurosci. **17:**7425–7432.
18. **Kwee, L., H. S. Baldwin, H. M. Shen, C. L. Stewart, C. Buck, C. A. Buck, and M. A. Labow.** 1995. Defective development of the embryonic and extraembryonic circulatory system in vascular cell adhesion molecule (VCAM-1) deficient mice. Development **121:**489–503.
19. **Lescisin, K. R., S. Varmuza, and J. Rossant.** 1988. Isolation and characterization of a novel trophoblast-specific cDNA in the mouse. Genes Dev. **2:**1639–1646.
20. **Lush, M. J., Y. Li, D. J. Read, A. C. Willis, and P. Glynn.** 1998. Neuropathy target esterase and a homologous *Drosophila* neurodegeneration-associated mutant protein contain a novel domain conserved from bacteria to man. Biochem. J. **332:**1–4.
21. **Moser, M., A. Pscherer, A. Imhof, R. Bauer, W. Amselgruber, F. Sinowatz, F. Hofstaedter, R. Schule, and R. Buettner.** 1995. Cloning and characterization of a second AP-2 transcription factor: AP-2 beta. Development **121:**2779–2788.
22. **Moser, M., A. Pscherer, C. Roth, J. Becker, G. Mucher, K. Zerres, C. Dixkens, J. Weis, L. Guay-Woodford, R. Buettner, and R. Fassler.** 1997. Enhanced apoptotic cell death of renal epithelial cells in mice lacking transcription factor AP-2β. Genes Dev. **1:**1938–1948.
23. **Moser, M., T. Stempfl, Y. Li, P. Glynn, R. Buttner, and D. Kretzschmar.** 2000. Cloning and expression of the murine sws/NTE gene. Mech. Dev. **90:**279–282.
24. **Sambrook, J., R. F. Fritsch, and T. Maniatis.** 1989. Molecular cloning: a laboratory manual, 2nd ed. Cold Spring Harbor Laboratory Press, Cold Spring Harbor, N.Y.
25. **Schluter, C., M. Duchrow, C. Wohlenberg, M. Becker, G. Key, H. D. Flad, and J. Gerdes, J.** 1993. The cell proliferation-associated antigen of antibody Ki-67: a very large, ubiquitous nuclear protein with numerous repeated elements, representing a new kind of cell cycle-maintaining proteins. J. Cell Biol. **123:**513–522.
26. **Schreiber, J., E. Riethmacher-Sonnenberg, D. Riethmacher, E. E. Tuerk, J. Enderich, M. R. Bösl, and M. Wegner.** 2000. Placental failure in mice lacking the mammalian homolog of glial cells missing, GCMa. Mol. Cell. Biol. **20:**2466–2474.
27. **Shalaby, F., J. Rossant, T. P. Yamaguchi, M. Gertsenstein, X.-F. Wu, M. L. Breitman, and A. Schuh.** 1995. Failure of blood-island formation and vasculogenesis in Flk-1 deficient mice. Nature **376:**62–66.
28. **Tanaka, M., M. Gertsenstein, J. Rossant, and A. Nagy.** 1997. Mash2 acts cell autonomously in mouse spongiotrophoblast development. Dev. Biol. **190:**55–65.
29. **Winrow, C. J., M. L. Hemming, D. M. Allen, G. B. Quistad, J. E. Casida, and C. Barlow.** 2003. Loss of neuropathy target esterase in mice links organophosphate exposure to hyperactivity. Nat. Genet. **33:**477–485.
30. **Yang, J. T., H. Rayborn, and R. O. Hynes.** 1995. Cell adhesion mediated by alpha-4 integrins are essential in placental and cardiac development. Development **121:**549–560.